ISSN 1063-7850, Technical Physics Letters, 2020, Vol. 46, No. 5, pp. 458–461. © Pleiades Publishing, Ltd., 2020.
Russian Text © The Author(s), 2020, published in Pis'ma v Zhurnal Tekhnicheskoi Fiziki, 2020, Vol. 46, No. 9, pp. 51–54.

Laser-Induced Graphene on a Polyimide Film: Observation of the Photon Drag Effect

K. G. Mikheev[a]*, R. G. Zonov[a], D. L. Bulatov[a], A. E. Fateev[a], and G. M. Mikheev[a]

[a] *Institute of Mechanics, Udmurt Federal Research Center, Ural Branch of the Russian Academy of Sciences, Izhevsk, 426067 Russia*

**e-mail: k.mikheev@udman.ru*

Received December 12, 2019; revised December 12, 2019; accepted February 18, 2020

Abstract—Film structures of porous graphene have been produced by irradiating a polyimide film with focused radiation of a continuous CO_2 laser. The generation of nanosecond photocurrent pulses induced by nanosecond laser pulses in a wide wavelength range has been observed in the obtained structures. It has been demonstrated that the photocurrent increases linearly with pulsed laser power and is an odd function of the angle of incidence of radiation on the film structure. The wavelength dependence of the coefficient of conversion of laser power into photocurrent has been measured. The obtained data have been interpreted as a result of current generation due to photon drag effect.

Keywords: laser-induced graphene, photocurrent, photon drag effect.

DOI: 10.1134/S1063785020050119

A considerable number of studies into the synthesis of graphene and its derivatives have already been published. Chemical-vapor deposition (CVD) is the best method for graphene production in terms of synthesis of a given number of monolayers, uniformity, and continuity [1, 2]. However, this method is too costly for industrial-scale production. The possibility of fabrication of porous graphene (3D graphene), which was called laser-induced graphene (LIG), by decomposition of a polymer film with pulse-periodic radiation of a CO_2 laser with a pulse duration of 14 μs in air under normal conditions has recently been demonstrated in [3]. This technique is rather simple to implement and allows one to form 3D graphene of arbitrary area and arbitrary shape rapidly on the surface of a carbon-containing material. In subsequent studies, LIG was synthesized with the use of CO_2 lasers generating pulse-periodic radiation with different pulse durations [4, 5], femtosecond laser pulses at 522 nm with a repetition rate of 1 MHz [6], and continuous radiation of a semiconductor laser with a wavelength of 405 nm [7]. LIG has already been found promising [8] for, e.g., fabrication of microsupercapacitors, sensors of various kinds, electrocatalysts, and microfluidic systems. At the same time, it is known that drag photocurrent [9–11], being an odd function of the radiation incidence angle (see, e.g., [12–14]), may be observed in graphene and nanographite films. However, as far as we know, no papers focused on the generation of photocurrent in LIG have been published to date. The aim of the present study is to observe and examine the photon drag effect (PDE) in LIG produced on the surface of a polyimide film with the use of a continuous CO_2 laser.

Commercial polyimide films with a thicknesses of 40, 80, and 120 μm and a CO_2 laser with a wavelength of 10.6 μm generating continuous radiation up to 50 W in power (the power could be adjusted smoothly) were used in our experiments on LIG synthesis. The laser power was measured with a PM100D meter (Thorlabs) with an S425C-L sensor head. LIG was formed in the process of line-by-line scanning by the focused laser beam on an automated stage performed in accordance with a preset program in air. The beam was focused by a lens with a focal distance of 51 mm onto the polyimide film surface. The diameter of the focused beam on the film was measured to be 190 μm using the well-known sharp edge method. The laser power and the scan rate were varied to find the optimum conditions of LIG fabrication. LIG was identified in the obtained films using a Horiba HR800 Raman spectrometer with an excitation radiation wavelength of 632.8 nm. The morphology of the obtained films was examined with a Leo 1550 Gemini (Zeiss) scanning electron microscope. The sheet resistance of films was determined using the four-probe method.

A special goniometric device was used to adjust radiation incidence angle α smoothly [13, 14] and, thus, examine the generation of photocurrent in films. Measurement electrodes (Fig. 1, inset) were secured to the studied film along its short sides and connected via a coaxial cable to a Tektronix TDS7704B digital

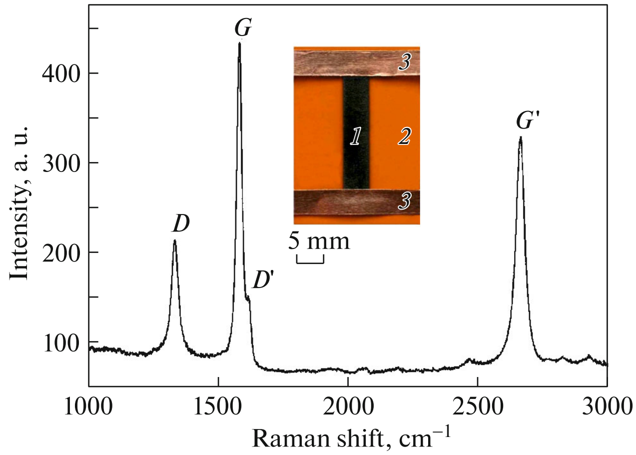

Fig. 1. Raman spectrum for laser-induced graphene. The inset shows (*1*) laser-induced graphene on (*2*) a polyimide film and (*3*) with electrodes.

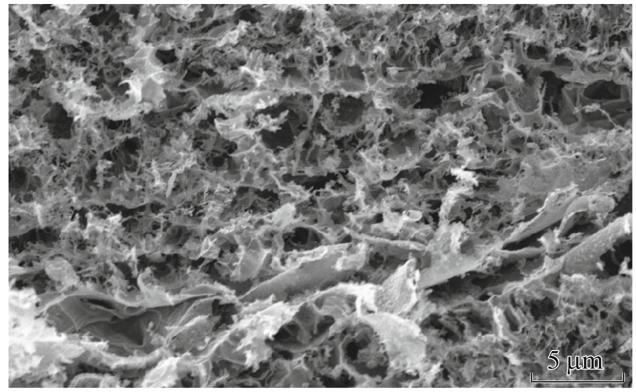

Fig. 2. SEM image of the surface of laser-induced graphene.

oscilloscope with a bandwidth of 7 GHz. The generation of photocurrent in the synthesized films was studied under irradiation with the first, second, third, and fourth harmonics of a single-mode YAG:Nd^{3+} laser with passive Q-factor modulation [15] at wavelengths λ_{in} = 1064, 532, 354.7, and 266 nm, respectively. The FWHM of laser pulses (τ_{in}) was measured with an SIR-5 photodetector (Thorlabs) and a digital oscilloscope. Energies E_{in} of nanosecond laser pulses incident on the studied films were measured by an ES111 pyroelectric energy sensor via a PM100USB (Thorlabs). The extreme values of voltage pulses U_x and FWHM τ pulse duration of single nanosecond photo-emf pulses generated between the measurement electrodes under oblique irradiation of the synthesized film were measured in experiments. Longitudinal photocurrent i_x flowing in the direction parallel to the incidence plane [13, 14] was determined as $i_x = U_x/r$, where r is the input impedance of the oscilloscope.

The experiments demonstrated that the following laser parameters are optimal for LIF fabrication: a power density of 8 W/cm^2 and a scan rate of 255 mm/s. The insert in Fig. 1 presents the photographic image of a rectangular film 5 × 20 mm in size. Its sheet resistance was 24 Ω/□. Figure 1 shows the Raman spectrum of the synthesized film with four primary lines: D (1330 cm^{-1}), D' (1616 cm^{-1}), G (1579 cm^{-1}), and G' (2660 cm^{-1}). Line G' is often called the "2D peak" (see, e.g., [2]). The first two scattering lines emerge due to the presence of defects in the hexagonal structure of sp^2 atoms, line G is related to the longitudinal oscillation mode of carbon atoms, and G' is the line of second-order Raman scattering by boundary phonons of the Brillouin zone [16, 17]. It is known that an intense G' line characterized by a single Lorentzian curve with an FWHM of 25 cm^{-1} and $I_{G'}/I_G > 1$, where $I_{G'}$ and I_G are the intensities of lines G' and G, is the distinguishing spectral feature of single-layer graphene [16]. As the number of layers increases, the G' line evolves into a complex of lines shifted in frequency relative to each other. The resulting G' line gets wider, and its primary peak shifts into the red region, while its intensity relative to that of the G line decreases considerably [16]. The G' line of the obtained spectrum is characterized by a single Lorentzian curve with an FWHM of 40 cm^{-1} and $I_{G'}/I_G = 0.7$. The frequency shift of line G' in the obtained spectrum is the same as that of line G' of graphene [16]. The $I_{G'}/I_G$ ratio, the frequency shift, the FWHM of line G' and the presence of line D' are all typical of multilayer graphene with rotational shift between its layers [16]. Note that the ratio of the intensities of lines D and G is 0.4. This suggests that the number of defects in graphene layers is low. According to [18], the in-plane size of crystallites (L_a) in a multilayer graphene depends on I_G/I_D and is written as L_a [nm] = $(2.4 \times 10^{-10})\lambda^4(I_G/I_D)$, where λ [nm] is the wavelength of radiation inducing Raman scattering. It follows from this formula that the in-plane size of crystallites in the studied LIG film is 108 nm.

The SEM image of the surface of the synthesized film (Fig. 2) reveals that this film has a porous petaline structure. The pores are up to several micrometers in size, and the thickness of petals is ~100 nm. Notably, these petals form an interconnected network, thus making the film highly conductive.

Experiments demonstrated that nanosecond photocurrent pulses are generated in the synthesized film structures under oblique irradiation with nanosecond laser pulses. For example, the photocurrent pulse duration at λ_{in} = 266 nm and τ_{in} = 9.4 ns is τ = 14.5 ns. The upper inset in Fig. 3 shows the linear dependence of photocurrent i_x on laser pulse power P_{in} at a wavelength of 1064 nm ($P_{in} = E_{in}/\tau_{in}$) and an incidence angle of –45°. Since this linear dependence of i_x on P_{in} is retained at photocurrent excitation wavelengths of 532, 354.7, and 266 nm, one may introduce coeffi-

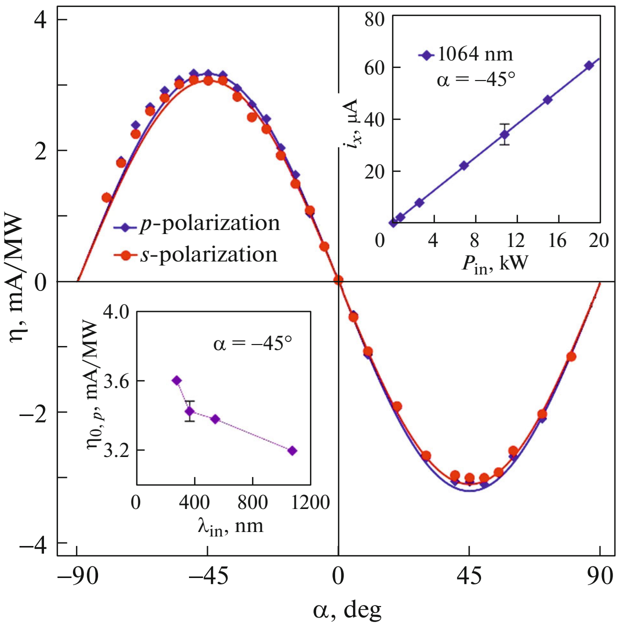

Fig. 3. Dependences of coefficient η of conversion of laser power into photocurrent on incidence angle α at a wavelength of 1064 nm for *s*- and *p*-polarized radiation incident on laser-induced graphene. The upper inset shows the dependence of LIG photocurrent on the power of *p*-polarized laser radiation with a wavelength of 1064 nm and an incidence angle of –45°. The lower inset shows the dependence of coefficient $\eta_{0,\,p}$ of conversion of laser power into LIG photocurrent on laser wavelength λ_{in}.

cient $\eta = i_x/P_{in}$ of conversion of laser power into photocurrent. Figure 3 presents the dependences of η on incidence angle α at a wavelength of 1064 nm for *s*- and *p*-polarized incident radiation. It can be seen that the photocurrent is zero under normal incidence of radiation and changes its direction when the sign of the incidence angle is reversed. The obtained sets of experimental data for *s*- and *p*-polarized incident radiation are closely approximated by dependence $\eta_{p(s)} = -\eta_{0,\,p(s)}\sin2\alpha$ (where $\eta_{0,\,p} \approx \eta_{0,\,s} \approx 3.4$ mA/MW) that is typical of the DE photocurrent in two-dimensional structures (see, e.g., [12]). The PDE current is normally generated together with the current induced by the surface photogalvanic effect (SPGE) [13, 14]. Angle dependences $\eta_p(\alpha)$ and $\eta_s(\alpha)$ for *p* and *s* polarizations are very close. This suggests that the longitudinal SPGE photocurrent, which vanishes in the case of *s*-polarized radiation [9, 19], is not generated in the synthesized film structures.

The lower inset in Fig. 3 demonstrates the experimental dependence of $\eta_{0,\,p}$ on excitation wavelength λ_{in}. It can be seen that conversion coefficient $\eta_{0,\,p}$ grows as λ_{in} decreases (i.e., as the energy of incident quanta increases). This agrees with the data for CVD nanographite films on silicon substrates [9, 20]. The nature of the obtained $\eta_{0,\,p}(\lambda_{in})$ dependence suggests that LIG may be used to detect laser radiation pulses in a wide spectral range.

Thus, a film structure of porous graphene may be synthesized on polyimide films irradiated by a continuous CO_2 laser operated at a wavelength of 10.6 μm with a power density of 8 W/cm^2 and a scan rate of 255 mm/s. PDE current is generated in laser-induced graphene under irradiation with nanosecond laser pulses in the 266–1064 nm wavelength range. Laser-induced graphene may be used to produce fast photodetectors for laser pulses with a wide operating spectral range.

ACKNOWLEDGMENTS

The authors wish to thank I.V. Reduto (St. Petersburg National Research Academic University, Russian Academy of Sciences) for his help in experiments. Equipment provided by the Center for Collective Use of Udmurt Federal Research Center (Ural Branch, Russian Academy of Sciences) was used in experiments.

FUNDING

This study was supported by the Russian Science Foundation, project no. 19-72-00071.

CONFLICT OF INTEREST

The authors declare that they have no conflict of interest.

REFERENCES

1. A. F. Vyatkin, Tech. Phys. Lett. **45**, 170 (2019).
2. A. B. Loginov, I. V. Bozh'ev, S. N. Bokova-Sirosh, E. D. Obraztsova, R. R. Ismagilov, B. A. Loginov, and A. N. Obraztsov, Tech. Phys. **64**, 1666 (2019).
3. J. Lin, Z. Peng, Y. Liu, F. Ruiz-Zepeda, R. Ye, E. L. G. Samuel, M. J. Yacaman, B. I. Yakobson, and J. M. Tour, Nat. Commun. **5**, 5714 (2014).
4. A. Lamberti, F. Perrucci, M. Caprioli, M. Serrapede, M. Fontana, S. Bianco, S. Ferrero, and E. Tresso, Nanotecnology **28**, 174002 (2017).
5. X. L. Duy, Z. Peng, Y. Li, J. Zhang, Y. Ji, and J. M. Tour, Carbon **126**, 472 (2018).
6. J. B. In, B. Hsia, J.-H. Yoo, J.-H. Yoo, S. Hyun, C. Carraro, R. Maboudian, and C. P. Grigoropoulos, Carbon **83**, 144 (2015).
7. J. Cai, C. Lv, and A. Watanabe, J. Mater. Chem. A **4**, 1671 (2016).
8. R. Ye, D. K. James, and J. M. Tour, Adv. Mater. **31**, e1803621 (2019).
9. P. A. Obraztsov, G. M. Mikheev, S. V. Garnov, A. N. Obraztsov, and Y. P. Svirko, Appl. Phys. Lett. **98**, 091903 (2011).
10. L. Zhu, Y. Huang, Z. Yao, B. Quan, L. Zhang, J. Li, C. Gu, X. Xu, and Z. Ren, Nanoscale **9**, 10301 (2017).

11. V. M. Kovalev, A. E. Miroshnichenko, and I. G. Savenko, Phys. Rev. B **98**, 165405 (2018).
12. E. V. Beregulin, P. M. Voronov, S. V. Ivanov, P. S. Kop'ev, and I. D. Yaroshetskii, JETP Lett. **59**, 85 (1994).
13. G. M. Mikheev, A. S. Saushin, V. M. Styapshin, and Y. P. Svirko, Sci. Rep. **8**, 8644 (2018).
14. G. M. Mikheev, A. S. Saushin, V. M. Styapshin, and Yu. P. Svirko, Tech. Phys. Lett. **44**, 844 (2018).
15. G. M. Mikheev, T. N. Mogileva, A. Yu. Popov, and D. G. Kalyuzhny, Instrum. Exp. Tech. **46**, 233 (2003).
16. A. C. Ferrari, J. C. Meyer, V. Scardaci, C. Casiraghi, M. Lazzeri, F. Mauri, S. Piscanec, D. Jiang, K. S. Novoselov, S. Roth, and A. K. Geim, Phys. Rev. Lett. **97**, 187401 (2006).
17. L. M. Malard, M. A. Pimenta, G. Dresselhaus, and M. S. Dresselhaus, Phys. Rep. **473**, 51 (2009).
18. L. G. Cançado, K. Takai, T. Enoki, M. Endo, Y. A. Kim, H. Mizusaki, A. Jorio, L. N. Coelho, R. Magalhães-Paniago, and M. A. Pimenta, Appl. Phys. Lett. **88**, 163106 (2006).
19. G. M. Mikheev, V. Ya. Kogai, R. G. Zonov, K. G. Mikheev, T. N. Mogileva, and Yu. P. Svirko, JETP Lett. **109**, 704 (2019).
20. G. M. Mikheev, R. G. Zonov, A. N. Obraztsov, A. P. Volkov, and Yu. P. Svirko, Tech. Phys. Lett. **31**, 94 (2005).

Translated by D. Safin